Physics-Informed Residual Attention GRU for Short-Term Six-DOF Platform Motion Prediction of Floating Offshore Wind Turbines

Xu Lin[1], Kai Zhao[2], Yingqi Pei[1], Yunling Ye[1,*], Kun Li[1] and Jin Gan[1]

[1]School of Naval Architecture, Ocean and Energy Power Engineering, Wuhan University of Technology, Wuhan 430063, P. R. China

[2]Wuhan Institute of Marine Electric Propulsion, Wuhan 430064, P. R. China

Abstract: Accurate short-term prediction of six-DOF platform motion is important for the state monitoring and health management of floating offshore wind turbines. This paper proposes a physics-informed residual attention GRU model, PI-Res Attn-GRU, for short-term six-DOF platform motion prediction. The model uses the preceding 10 s of platform motion to predict the subsequent 5 s. First, a GRU temporal encoder transforms the historical six-DOF motion sequence into a sequence of hidden representations. An Attention-Last State Fusion Module then combines an attention-pooled feature capturing key historical dynamics with the final hidden state representing the latest motion state, thereby forming a context representation for future prediction. A Step-Delta incremental decoder starts from the last observed state and recursively predicts motion increments to generate the future motion sequence. In addition, physics-informed constraint terms are incorporated into the training loss to promote boundary position continuity, initial velocity consistency, and acceleration smoothness. Experiments are conducted on 22 floating offshore wind turbine simulation cases. An eight-fold leave-one-wind-speed-out cross-validation procedure is applied to the development set for model selection, while cases at wind speeds of 8, 16, and 24 m/s are held out exclusively for testing. The final model achieves an MAE of 0.0333, an MSE of 0.0046, an RMSE of 0.0681, and an R^2 of 0.9939 on the test set. Compared with LSTM, the best-performing baseline model, PI-Res Attn-GRU reduces the MAE, MSE, and RMSE by 54.1%, 72.0%, and 47.1%, respectively. The results demonstrate that the proposed model can accurately predict short-term six-DOF platform motion and generalize well across different operating conditions.

Keywords: Floating offshore wind turbine, short-term prediction, physics-informed learning, motion response.

1. INTRODUCTION

Floating offshore wind turbines are subjected to the coupled effects of wind, waves, currents, mooring systems, and control systems. These factors lead to complex six-DOF motion responses. Platform motion not only affects aerodynamic performance and power generation stability, but is also closely related to structural safety. Reliability assessment and health management of floating offshore wind turbines have therefore received increasing attention [1-6]. Accurate short-term platform-motion prediction can therefore provide valuable state information for reliability assessment and health management of floating offshore wind turbines.

In recent years, data-driven methods have increasingly been applied to dynamic-response prediction of floating offshore wind turbines [7-9]. Shi *et al*. [10] proposed a short-term motion prediction method for floating offshore wind turbines based on a multi-input LSTM neural network, which improved the representation of nonlinear temporal features in platform motion. On this basis, He *et al*. [11] further investigated short-term motion prediction of floating offshore wind turbines during shutdown, showing that deep learning models can learn short-term motion evolution patterns from historical motion responses.

For wave-induced platform motions, Yin *et al*. [12] used a Bi-LSTM model to predict wave-induced motion of a deepwater floating offshore wind turbine platform. Bidirectional temporal modeling improved feature extraction under complex wave loading. Song *et al*. [13] incorporated time-frequency feature fusion and signal decomposition into short-term FOWT motion prediction, which further improved the representation of nonstationary motion signals.

As deep temporal models have evolved, attention mechanisms have also been introduced into floating offshore wind turbine motion prediction [14-16]. Chen *et al*. [17] proposed an attention-based machine learning method for short-term motion prediction of floating offshore wind turbines, which can adaptively focus on key temporal features in the historical sequence that are most relevant to future motion responses, thus improving multi-step prediction performance. In addition to overall platform motion, Chen *et al*. [18] investigated deep-learning-based prediction of floating offshore wind turbine pitch responses and showed that neural networks can effectively learn the nonlinear mapping in platform attitude responses. Wang *et al*. [19] developed a deep-learning method to identify floating wind turbine tower responses. The method supports structural-response estimation in monitoring systems and further demonstrates the potential of data-driven models in state estimation and response prediction of floating offshore wind turbines.

*Address correspondence to this author at the School of Naval Architecture, Ocean and Energy Power Engineering, Wuhan University of Technology, Wuhan 430063, P. R. China; E-mail: yeyunling@whut.edu.cn

Received on 09-07-2026 Accepted on 24-08-2026 Published on 27-08-2026

Viewed comparatively, the related studies differ mainly in three respects. First, their prediction targets range from one or several platform-motion components to tower structural responses, resulting in different output dimensions and task definitions. Second, their inputs range from historical motion sequences to multi-source combinations involving environmental conditions and structural-response information. Third, their modeling strategies enhance temporal representation through recurrent architectures, bidirectional encoding, signal decomposition, hybrid feature extraction, or attention mechanisms. Because the datasets, input variables, prediction targets, operating conditions, and forecast horizons differ among these studies, their reported numerical results are not directly comparable. Instead, their contributions are complementary: some enrich the available input information, some improve temporal feature extraction, and others extend data-driven prediction to specific response variables or operating scenarios.

Despite these advances, two limitations remain in existing studies. First, many studies focus on predicting a single platform motion component, whereas simultaneous short-term prediction of all six degrees of freedom (six-DOF) has received comparatively limited attention. Second, most existing models are optimized primarily for prediction accuracy, with few explicit constraints on boundary continuity and dynamic smoothness. Consequently, multi-step predictions may not connect smoothly with the last historical observation and may exhibit unrealistic fluctuations. Therefore, a unified six-DOF prediction method that combines effective temporal feature extraction with continuous and dynamically smooth sequence generation is needed.

To address these limitations, this study develops a physics-informed residual attention GRU model, termed PI-Res Attn-GRU, for short-term six-DOF motion prediction of floating offshore wind turbine platforms. The model uses the preceding 10 s of platform motion to predict the subsequent 5 s. A GRU temporal encoder first transforms the historical motion sequence into a sequence of hidden representations. An Attention-Last State Fusion Module then combines an attention-pooled representation of key historical dynamics with the final hidden state representing the latest encoded motion state. Based on the resulting context representation, a Step-Delta incremental decoder starts from the last observed state and recursively predicts motion increments to generate the future sequence. In addition, physics-informed terms for boundary position continuity, initial velocity consistency, and acceleration smoothness are incorporated into the training loss.

The main contributions of this study are as follows:

(i) A unified prediction framework is established for the simultaneous short-term prediction of all six platform motion components from historical six-DOF motion sequences.

(ii) An Attention-Last State Fusion Module is developed to combine key historical dynamics with the latest encoded motion state, while a Step-Delta incremental decoder generates the future sequence recursively from the last observation.

(iii) Physics-informed constraint terms are incorporated into the training loss to promote a smooth connection between the historical and predicted sequences and improve the dynamic smoothness of multi-step predictions.

(iv) The proposed model is comprehensively evaluated using 22 OpenFAST simulation cases. Its cross-condition performance is examined through leave-one-wind-speed-out cross-validation, an independent test set, comparisons with four baseline models, and sensitivity analyses of the prediction horizon and input-window length.

The remainder of this paper is organized as follows. Section 2 presents the OpenFAST simulation model, the design of the simulation cases, and the architecture and loss function of PI-Res Attn-GRU. Section 3 describes the experimental settings and reports the cross-validation results, model comparisons, representative six-DOF predictions, error distributions, and performance under different test wind speeds. Section 4 investigates the sensitivity of the model to the prediction horizon and input-window length. Finally, Section 5 summarizes the main findings, discusses the limitations, and outlines directions for future research.

2. METHODOLOGY

2.1. Simulation Model

Figure **1** shows the overall structure and principal dimensions of the 5-MW OC4-DeepCwind semi-submersible floating offshore wind turbine considered in this study. Numerical simulations are conducted using OpenFAST under coupled wind-wave conditions. The system consists of a rotor, nacelle, tower, semi-submersible floating platform, and mooring system, thereby capturing the coupled multibody dynamics of a floating offshore wind turbine. Wind loads act on the rotor and tower system, while wave loads act on the semi-submersible floating platform. The mooring system constrains the platform. Under combined wind and wave actions, the platform undergoes six-DOF motions, including surge, sway, heave, roll, pitch, and yaw.

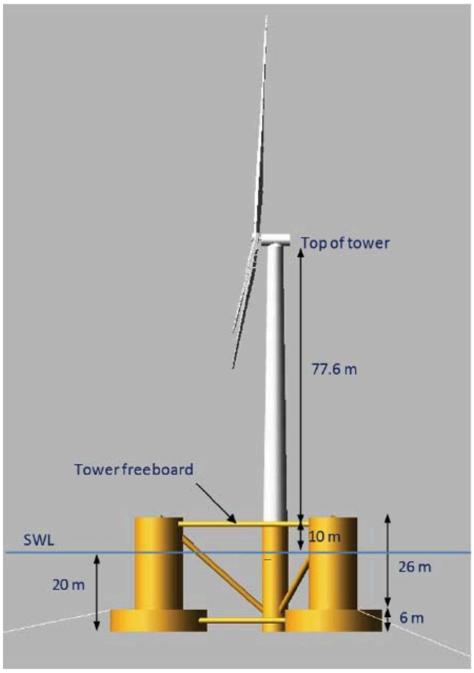

Figure 1: Overall structure of the 5 MW OC4-DeepCwind FOWT.

2.2. Design of Simulation Cases

To construct a dataset for short-term six-DOF platform motion prediction of floating offshore wind turbines, typical coupled wind-wave cases are selected based on IEC design load cases [20]. Numerical simulations are then carried out. In this paper, DLC1.1 and DLC1.6 are selected as the main research cases. DLC1.1 represents typical operating conditions under normal turbulent wind. DLC1.6 represents extreme sea states with stronger wave loading. These two types of cases cover FOWT motion responses under different wind speeds and wave intensities. Therefore, they can be used to build a dataset spanning distinct operating conditions. The detailed design load case matrix is shown in Table **1**.

2.3. PI-Res Attn-GRU Model Structure

Figure **2** shows the overall framework of the proposed PI-Res Attn-GRU model.

The historical six-DOF platform motion sequence is first fed into a GRU temporal encoder to obtain a sequence of hidden representations. Next, an Attention-Last State Fusion Module combines two complementary representations: an attention-pooled feature that captures key historical dynamics and the final hidden state that represents the latest encoded motion state. The fused context representation is then passed to the Step-Delta incremental decoder, which recursively predicts motion increments from the last observed state to generate the future six-DOF platform motion sequence. During training, physics-informed constraint terms for boundary position continuity, initial velocity consistency, and acceleration smoothness are incorporated into the loss function.

The PI-Res Attn-GRU model takes the historical six-DOF platform motion response as input and predicts the future platform motion response over a short horizon. Let the six-DOF platform motion vector at time *t* be defined as:

$$\mathbf{q}_t = [x_t, y_t, z_t, \phi_t, \theta_t, \psi_t] \in \mathbb{R}^6 \tag{1}$$

In this vector, x_t, y_t, z_t denote the translational motions of surge, sway, and heave, respectively. ϕ_t, θ_t, ψ_t denote the rotational motions of roll, pitch, and yaw, respectively. The model input is the motion sequence over the past T_{in} time steps:

Table 1: IEC Design Load Case Matrix

	DLC		DLC1.1		DLC1.6	
Wind speed (m/s)	Hs (m)	Tp (s)	γ (-)	Hs (m)	Tp (s)	γ (-)
4	1.10	8.52	1.00	6.30	11.50	2.75
6	1.18	8.31	1.00	8.00	12.70	2.75
8	1.32	8.01	1.00	8.00	12.70	2.75
10	1.54	7.65	1.00	8.10	12.80	2.75
12	1.84	7.44	1.00	8.50	13.10	2.75
14	2.19	7.46	1.00	8.50	13.10	2.75
16	2.60	7.64	1.35	9.80	14.10	2.75
18	3.06	8.05	1.59	9.80	14.10	2.75
20	3.63	8.52	1.82	9.80	14.10	2.75
22	4.03	8.99	1.82	9.80	14.10	2.75
24	4.52	9.45	1.89	9.80	14.10	2.75

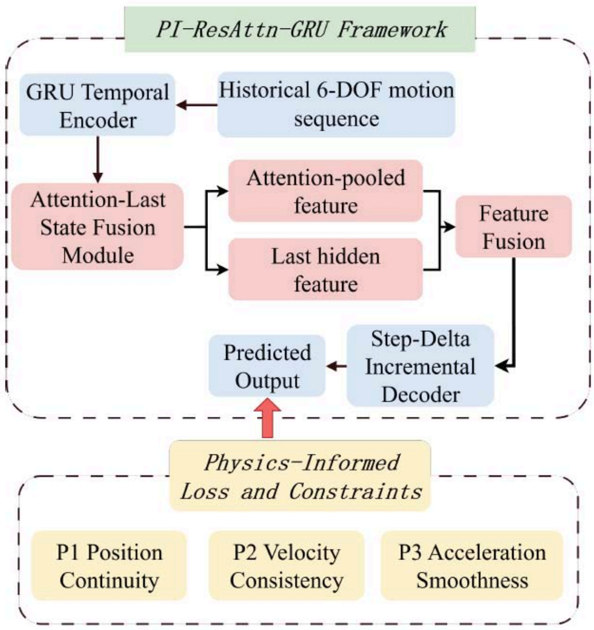

Figure 2: Architecture of the proposed PI-Res Attn-GRU model.

$$\mathbf{X}_t = [\mathbf{q}_{t-T_{in}+1}, \mathbf{q}_{t-T_{in}+2}, \cdots, \mathbf{q}_t] \in \mathbb{R}^{T_{in}\times 6} \quad (2)$$

The sampling frequency is 20 Hz, and the input window length is 10 s. Therefore, $T_{in} = 200$. The model output is the predicted sequence over the future T_{out} time steps:

$$\hat{\mathbf{Y}}_t = [\hat{\mathbf{q}}_{t+1}, \hat{\mathbf{q}}_{t+2}, \cdots, \hat{\mathbf{q}}_{t+T_{out}}] \in \mathbb{R}^{T_{out}\times 6} \quad (3)$$

The prediction horizon is 5 s; therefore, T_{out}=100. First, the input sequence $\boldsymbol{X}_t$ is fed into the GRU temporal encoder. The encoder is used to extract temporal dependencies from the historical platform motion. Its hidden state update can be expressed as:

$$\mathbf{h}_i = \mathrm{GRU}(\mathbf{q}_i, \mathbf{h}_{i-1}) \quad (4)$$

After encoding, the hidden state sequence is obtained as:

$$\mathbf{H} = [\mathbf{h}_1, \mathbf{h}_2, \cdots, \mathbf{h}_{T_{in}}] \quad (5)$$

Then, an Attention-Last State Fusion Module is used to extract key temporal features. On the one hand, the attention mechanism assigns an importance weight to the hidden state at each time step:

$$e_i = f_{attn}(\mathbf{h}_i), \alpha_i = \frac{\exp(e_i)}{\sum_{j=1}^{T_{in}} \exp(e_j)} \quad (6)$$

The attention-pooled feature is then obtained as:

$$\mathbf{m}_{attn} = \sum_{i=1}^{T_{in}} \alpha_i \, \mathbf{h}_i \quad (7)$$

On the other hand, the hidden state at the last time step is retained:

$$\mathbf{m}_{last} = \mathbf{h}_{T_{in}} \quad (8)$$

Here, $\mathbf{m}_{attn}$ encodes the key dynamic information in the historical sequence, and $\mathbf{m}_{last}$ denotes the latest motion state at the current time. These two features are concatenated and mapped through a linear layer to obtain the fused feature:

$$\mathbf{c} = \mathbf{W}_c[\mathbf{m}_{attn}; \mathbf{m}_{last}] + \mathbf{b}_c \quad (9)$$

In the decoding stage, a Step-Delta incremental decoder is used. Rather than directly producing the complete future motion sequence, the decoder starts from the last historical state and predicts future motion increments step by step:

$$\Delta\hat{\mathbf{q}}_{t+k} = g(\mathbf{c}, \Delta\hat{\mathbf{q}}_{t+k-1}, \mathbf{s}_{k-1}) \quad (10)$$

$$\hat{\mathbf{q}}_{t+k} = \hat{\mathbf{q}}_{t+k-1} + \Delta\hat{\mathbf{q}}_{t+k}, k = 1,2,\cdots, T_{out} \quad (11)$$

Here, g denotes the increment-prediction function implemented by a GRU cell and fully connected layers. $\mathbf{s}_{k-1}$ is the decoder hidden state, and $\hat{\boldsymbol{q}}_t = \boldsymbol{q}_t$. This recursive incremental prediction strategy can improve the continuity of the future motion sequence. This strategy is suitable for short-term prediction of continuous dynamic responses such as platform motion.

During model training, the loss function consists of the data loss and the physics-informed constraint loss:

$$\mathcal{L} = \mathcal{L}_{data} + \lambda_1 P_1 + \lambda_2 P_2 + \lambda_3 P_3 \quad (12)$$

Here, $\mathcal{L}_{data}$ is the mean squared error between the predicted sequence and the true sequence. P_1, P_2, P_3 denote the constraints of position continuity, initial velocity consistency, and acceleration smoothness, respectively:

$$P_1 = \|\hat{\mathbf{q}}_{t+1} - \mathbf{q}_t\|_2^2 \quad (13)$$

$$P_2 = \|(\hat{\mathbf{q}}_{t+1} - \mathbf{q}_t) - (\mathbf{q}_t - \mathbf{q}_{t-1})\|_2^2 \quad (14)$$

$$P_3 = \sum_{k=2}^{T_{out}} \|\hat{\mathbf{q}}_{t+k} - 2\hat{\mathbf{q}}_{t+k-1} + \hat{\mathbf{q}}_{t+k-2}\|_2^2 \quad (15)$$

3. EXPERIMENTAL RESULTS

3.1. Experimental Settings and Evaluation Metrics

To validate the effectiveness of the proposed PI-Res Attn-GRU model in short-term platform motion prediction of floating offshore wind turbines, experiments were conducted based on the simulation cases described in Section 2. For data splitting, a wind-speed-based splitting strategy was used to evaluate the generalization ability of the model under different operating conditions. The cases with wind speeds of 4, 6, 10, 12, 14, 18, 20, and 22 m/s were used as the development set. The three test wind speeds were selected to cover the lower, intermediate, and upper portions of the simulated wind-speed range and to examine different forms of cross-condition generalization. The 8 and 16 m/s conditions are each bracketed by neighboring wind speeds in the development set and therefore evaluate interpolation to unseen wind-speed conditions. The 24 m/s condition lies at the upper boundary of the simulated range and exceeds the maximum development wind speed of 22 m/s, thereby evaluating extrapolation under a high-wind condition. Both DLC1.1 and DLC1.6 were retained at each test wind speed to cover normal turbulent operation and stronger wave-loading conditions. The cases with wind speeds of 8, 16, and 24 m/s were used as the held-out test set. The held-out test set was not used for model training, parameter tuning, or model selection. Within the development set, a leave-one-wind-speed-out cross-validation strategy was adopted. In each run, one development wind speed was selected as the validation condition, and the remaining development wind speeds were used as training conditions. This strategy was used to evaluate the stability of the model under different wind speed conditions.

In this paper, four metrics are used to evaluate the prediction performance of the model: MAE, MSE, RMSE, and R^2. MAE represents the mean absolute error between the predicted values and the true values. It can directly reflect the overall prediction bias of the model. MSE represents the mean squared error and is more sensitive to large errors. RMSE is the square root of MSE. It has the same unit as the original variable and is suitable for measuring the overall prediction error. R^2 is used to measure the ability of the model to explain the variation in the true response. A value closer to 1 indicates that the predicted results are closer to the true values. The four evaluation metrics are defined as follows:

$$MAE = \frac{1}{N}\sum_{i=1}^{N}|y_i - \hat{y}_i| \tag{16}$$

$$MSE = \frac{1}{N}\sum_{i=1}^{N}(y_i - \hat{y}_i)^2 \tag{17}$$

$$RMSE = \sqrt{\frac{1}{N}\sum_{i=1}^{N}(y_i - \hat{y}_i)^2} \tag{18}$$

$$R^2 = 1 - \frac{\sum_{i=1}^{N}(y_i - \hat{y}_i)^2}{\sum_{i=1}^{N}(y_i - \bar{y})^2} \tag{19}$$

Here, y_i denotes the true value, $\hat{y}_i$ denotes the predicted value of the model, $\bar{y}$ denotes the mean value of the true values, and N denotes the total number of test samples. These metrics are used together to evaluate the error magnitude, predictive accuracy, and ability of the model to reproduce trends in platform-motion responses.

3.2. Cross-Validation Results

An eight-fold leave-one-wind-speed-out cross-validation was performed on the development set to evaluate the stability of PI-Res Attn-GRU and determine the final training epoch. In each fold, one wind-speed condition was used for validation, while the remaining seven conditions were used for training. Figure **3** presents the training and validation loss curves obtained during cross-validation. As shown in Figure **3**, both losses decrease rapidly during the early epochs and gradually stabilize after approximately 30 epochs. No persistent increase in the validation loss is observed, indicating stable model convergence. Across the eight folds, the model achieves an average MAE of 0.0325 ± 0.0054, an MSE of 0.0044 ± 0.0013, an RMSE of 0.0652 ± 0.0104, and an R^2 of 0.9923 ± 0.0029.

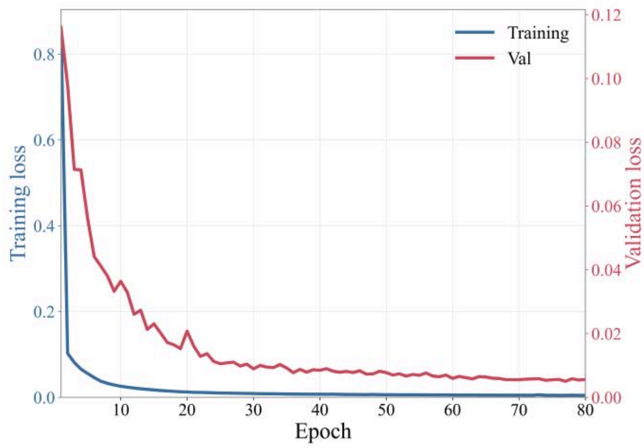

Figure 3: Cross-validation loss curves.

3.3. Test-Set Model Comparison

To further evaluate the prediction performance of the proposed model, PI-Res Attn-GRU was compared with TCN, RNN, Transformer, and LSTM on the test set containing wind-speed conditions of 8, 16, and 24 m/s. The four baseline models represent different sequence-modeling paradigms: convolution-based temporal modeling (TCN), conventional recurrent modeling (RNN), self-attention-based modeling (Transformer), and gated recurrent modeling (LSTM). All models were evaluated under the same experimental settings, with a 10-s input window and a 5-s prediction horizon. Figure **4** compares their test-set performance in terms of MAE, MSE, RMSE, and R^2.

As shown in Figure **4**, PI-Res Attn-GRU achieves the best performance, with an MAE of 0.0333, an MSE of 0.0046, an RMSE of 0.0681, and an R^2 of 0.9939. LSTM is the strongest baseline, obtaining an MAE of 0.0726, an MSE of 0.0166, an RMSE of 0.1288, and an R^2 of 0.9781. Compared with LSTM, the proposed model reduces the MAE, MSE, and RMSE by 54.1%,

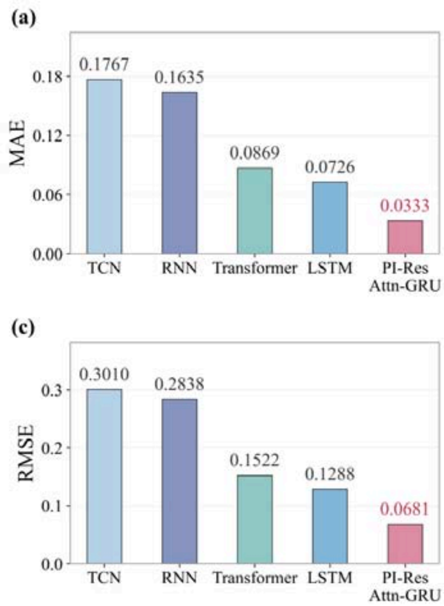

Figure 4: Test-set performance comparison.

72.0%, and 47.1%, respectively, while increasing R² by 0.0158. These results demonstrate that PI-Res Attn-GRU is more accurate and generalizes better across operating conditions.

3.4. Visualization of Prediction Results

To provide an intuitive evaluation of the prediction performance, a representative test case is selected for visualization. Figure **5** shows the six-DOF prediction results of the proposed model under the DLC1.1 case with a wind speed of 16 m/s. The black curves represent the historical input sequence over the past 10 s. The blue dashed curves represent the true future motion responses over the next 5 s, and the red curves represent the predicted results of the proposed model.

As shown in Figure **5**, the predicted curves are generally close to the true curves in all six motion directions. The model can capture the main variation trends of surge, sway, heave, roll, pitch, and yaw. In addition, the predicted curves remain continuous at the start of the forecast. This indicates that the proposed model produces stable short-term predictions and effectively tracks the future evolution of platform motion.

3.5. Prediction Error Distribution of Six-DOF Motion

The prediction errors of the model for the six-DOF motion responses on the test set are shown in Table **2**. Overall, the model achieves high prediction accuracy in

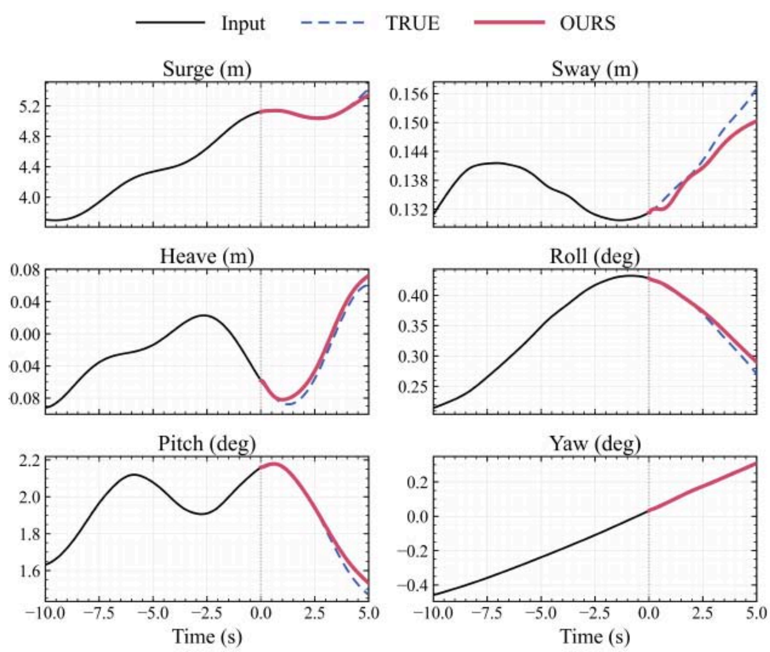

Figure 5: Visualization of prediction results.

Table 2: Prediction Error Distribution of Six-DOF Motion

DOF	MAE	MSE	RMSE	R^2
Surge	0.0637	0.0092	0.0963	0.9956
Sway	0.0049	0.00006	0.0078	0.9995
Heave	0.0308	0.0025	0.0506	0.9939
Roll	0.0111	0.0003	0.0191	0.9917
Pitch	0.0748	0.0150	0.1227	0.9759
Yaw	0.0142	0.0004	0.0219	0.9995

all six degrees of freedom. The R^2 values of all motion directions are higher than 0.97. This indicates that the model accurately reproduces trends in the multi-DOF platform motion responses.

For the translational degrees of freedom, the model produces the smallest prediction error in the sway direction. The MAE is only 0.0049, the RMSE is 0.0078, and the R^2 reaches 0.9995. This shows that the model can accurately capture the short-term motion variation in this direction. Prediction in the heave direction is also accurate, with an RMSE of 0.0506 and an R^2 of 0.9939. In contrast, the error in the surge direction is larger, with an RMSE of 0.0963. However, its R^2 still reaches 0.9956. This indicates that the model can still closely track the overall trend in this direction.

For the rotational degrees of freedom, performance is strongest in the yaw and roll directions. The RMSE and R^2 in the yaw direction are 0.0219 and 0.9995, respectively. The RMSE and R^2 in the roll direction are 0.0191 and 0.9917, respectively. These results indicate that the model accurately predicts the short-term responses in these two rotational directions. The pitch direction has the largest relative error, with an MAE of 0.0748, an RMSE of 0.1227, and an R^2 of 0.9759.

The results for the six degrees of freedom show that the PI-Res Attn-GRU model accurately predicts overall platform motion. It can also maintain stable performance across the motion components. The highest prediction accuracy is observed in the sway and yaw directions. The pitch direction is the most challenging component to predict, but its R^2 remains at a high level. These results show that the proposed model can effectively learn the temporal evolution of six-DOF platform motion responses and performs well in short-term multi-DOF prediction.

3.6. Prediction Results Under Different Test Wind Speeds

To assess the generalization of the proposed model under different wind speed conditions, performance was evaluated at three held-out test wind speeds: 8, 16, and 24 m/s. The results are shown in Table **3**.

As shown in Table **3**, the model achieves high prediction accuracy under all three held-out test wind speeds. The lowest prediction error is obtained under the 8 m/s condition. The MAE is 0.0249, the RMSE is 0.0517, and the R^2 reaches 0.9956. This indicates that the model accurately predicts the platform motion response under low wind speed conditions. As the wind speed increases, the amplitude and dynamic complexity of the platform motion response also increase. The prediction error therefore increases accordingly. Under the 16 m/s condition, the model achieves an RMSE of 0.0720 and an R^2 of 0.9936. Under the high wind speed condition of 24 m/s, the RMSE is 0.0777, and the R^2 remains 0.9916.

Overall, although the prediction error increases slightly with wind speed, the R^2 values remain high under all test wind speeds. This shows that the model accurately captures trends in six-DOF platform motion responses under different wind speed conditions. These results indicate that the proposed PI-Res Attn-GRU model remains stable and generalizes well to unseen wind-speed conditions.

4. SENSITIVITY ANALYSIS

4.1. Prediction-Horizon Sensitivity

To evaluate the long-horizon extrapolation capability of PI-Res Attn-GRU, the input window was fixed at 10 s, while the prediction horizon was extended

Table 3: Prediction Results under Different Test Wind Speeds

Wind speed	MAE	MSE	RMSE	R^2
8 m/s	0.0249	0.0026	0.0517	0.9956
16 m/s	0.0344	0.0051	0.0720	0.9936
24 m/s	0.0405	0.0060	0.0777	0.9916

Table 4: Performance under Different Prediction Horizons

Prediction horizon (s)	MAE	MSE	RMSE	R^2
5	0.0333	0.0046	0.0681	0.9939
6	0.0433	0.0081	0.0902	0.9892
7	0.0583	0.0167	0.1292	0.9779
8	0.0818	0.0392	0.1981	0.9481
9	0.1149	0.0882	0.2970	0.8834
10	0.1566	0.1757	0.4191	0.7677

Table 5: Performance under Different Input-Window Lengths

Input-window length (s)	MAE	MSE	RMSE	R^2
2	0.3163	0.7156	0.8459	0.0538
4	0.1739	0.1831	0.4280	0.7578
6	0.1162	0.0806	0.2840	0.8933
8	0.0699	0.0274	0.1655	0.9637
10	0.0333	0.0046	0.0681	0.9939

from 5 s to 10 s. The trained PI-Res Attn-GRU model and its normalization parameters were kept unchanged, and identical forecast origins were used for all prediction horizons. Therefore, this experiment evaluates the recursive prediction limit of the final model rather than the performance of separately retrained models.

As shown in Table **4**, the model maintains high accuracy within a prediction horizon of 5–7 s, with the R^2 decreasing only from 0.9939 to 0.9779. When the horizon reaches 8 s, the RMSE increases to 0.1981 and the R^2 decreases to 0.9481. A more substantial degradation is observed at 9 and 10 s, where the R^2 decreases to 0.8834 and 0.7677, respectively. This deterioration is mainly caused by the accumulation of incremental errors in the recursive Step-Delta decoder. Although the physics-informed constraints improve local continuity and smoothness, they cannot completely prevent long-term phase drift. Therefore, the current model provides reliable, high-accuracy predictions over horizons of approximately 5–7 s, while predictions beyond 8 s should be used with greater caution.

4.2. Input-Window Sensitivity

To investigate the influence of historical information on prediction performance, the prediction horizon was fixed at 5 s, while the input window was set to 2, 4, 6, 8, and 10 s. The same trained PI-Res Attn-GRU model, test cases, normalization parameters, and forecast origins were used for all settings. Only the length of the historical sequence provided during inference was changed.

Table **5** shows a clear improvement in prediction performance as the input-window length increases. With only 2 s of historical motion data, the model achieves an R^2 of 0.0538, indicating that this window is too short to adequately capture the coupled oscillatory dynamics of six-DOF platform motion. Increasing the input window to 6 and 8 s raises the R^2 to 0.8933 and 0.9637, respectively. The 10-s input window provides the best overall performance, with an MAE of 0.0333, an MSE of 0.0046, an RMSE of 0.0681, and an R^2 of 0.9939. These results indicate that longer historical sequences provide more complete information about motion cycles and temporal dependencies, thereby improving future-motion prediction. Because the model was trained using a 10-s input window, the performance degradation observed with shorter input sequences reflects its sensitivity to reduced historical information rather than differences among separately retrained models. Therefore, the 10-s input window is retained for the current model configuration.

5. CONCLUSION

This study addressed the simultaneous short-term prediction of all six degrees of freedom (six-DOF) of floating offshore wind turbine platforms and developed a physics-informed residual attention GRU model, PI-Res Attn-GRU. The model integrates a GRU temporal encoder, an Attention-Last State Fusion Module, and a Step-Delta incremental decoder. Physics-informed constraints are incorporated to promote position continuity at the forecasting boundary, initial-velocity consistency, and acceleration smoothness. The model was evaluated using 22 OpenFAST simulation cases. Leave-one-wind-speed-out cross-validation was performed on the development set, while cases at wind speeds of 8, 16, and 24 m/s were used as an independent test set.

(1) PI-Res Attn-GRU demonstrated stable simultaneous six-DOF prediction performance across different wind-speed conditions in the development set. During cross-validation, the model achieved an average MAE of 0.0325 ± 0.0054 and an average R^2 of 0.9923 ± 0.0029. These results indicate that the model maintains stable prediction performance across the evaluated development conditions.

(2) The proposed model achieved the best overall prediction performance on the test set. PI-Res Attn-GRU obtained an MAE of 0.0333, an MSE of 0.0046, an RMSE of 0.0681, and an R^2 of 0.9939. Compared with LSTM, the best-performing baseline model, PI-Res Attn-GRU reduced the MAE, MSE, and RMSE by 54.1%, 72.0%, and 47.1%, respectively, while increasing R^2 by 0.0158. These results demonstrate that PI-Res Attn-GRU provides higher prediction accuracy and goodness of fit under the unseen test wind-speed conditions.

(3) The prediction-horizon analysis identified the effective range of the recursive forecasting strategy. With the input window fixed at 10 s, R^2 remained at 0.9779 for a 7-s prediction horizon but decreased to 0.7677 when the prediction horizon reached 10 s. Therefore, the current model maintains high prediction accuracy over horizons of approximately 5-7 s, whereas the accumulation of recursive errors leads to a clear deterioration in performance as the prediction horizon increases further.

(4) The input-window analysis quantified the influence of historical information on prediction performance. With the prediction horizon fixed at 5 s, increasing the input window from 2 to 10 s reduced the MAE from 0.3163 to 0.0333. This result indicates that sufficient historical motion information helps the model capture the coupled oscillatory characteristics of six-DOF platform motion and improves future-motion prediction accuracy under the current model configuration.

Overall, PI-Res Attn-GRU achieved accurate and stable simultaneous six-DOF motion prediction under the evaluated simulation conditions. The prediction-horizon and input-window analyses further established the effective operating range of the model under its current configuration. The proposed method can support short-term platform motion-state estimation and subsequent state-monitoring studies for floating offshore wind turbines.

The present validation is primarily based on OpenFAST simulation cases, and the model inputs contain only historical platform-motion information. Moreover, prediction performance decreases at longer horizons because of recursive error accumulation. Future work will incorporate wind-wave environmental variables and structural-load information, quantify prediction uncertainty, and evaluate the model under broader operating conditions and using measured operational data to further improve its reliability and engineering applicability.

FUNDING

The authors acknowledge projects supported by the Open Fund of Key Laboratory of High Performance Ship Technology (Wuhan University of Technology), Ministry of Education (No. gxnc25112201), the Hubei Provincial Natural Science Foundation of China (2026AFB224) and the China Postdoctoral Science Foundation under Grant Number 2025M780268.

AUTHOR CONTRIBUTIONS

Xu Lin: Conceptualization, Methodology, Formal analysis, Validation, Writing – original draft. Kai Zhao: Investigation, Data curation, Validation, Visualization. Yingqi Pei: Investigation, Methodology, Validation. Yunling Ye: Conceptualization, Methodology, Supervision, Project administration, Writing – review & editing. Kun Li: Software, Validation, Visualization. Jin Gan: Supervision, Resources, Funding acquisition, Writing – review & editing.

CONFLICTS OF INTEREST

No conflict of interest.

REFERENCES

[1] Li H, Diaz H, Guedes Soares C. A developed failure mode and effect analysis for floating offshore wind turbine support structures. Renewable Energy 2021; 164: 133-145. https://doi.org/10.1016/j.renene.2020.09.033

[2] Li H, Díaz H, Guedes Soares C. A failure analysis of floating offshore wind turbines using AHP-FMEA methodology. Ocean Engineering 2021; 234: 109261. https://doi.org/10.1016/j.oceaneng.2021.109261

[3] Li H, Guedes Soares C, Huang H-Z. Reliability analysis of a floating offshore wind turbine using Bayesian Networks. Ocean Engineering 2020; 217: 107827. https://doi.org/10.1016/j.oceaneng.2020.107827

[4] Li H, Guedes Soares C. Assessment of failure rates and reliability of floating offshore wind turbines. Reliability Engineering & System Safety 2022; 228: 108777. https://doi.org/10.1016/j.ress.2022.108777

[5] Li H, Huang C-G, Guedes Soares C. A real-time inspection and opportunistic maintenance strategies for floating offshore wind turbines. Ocean Engineering 2022; 256: 111433. https://doi.org/10.1016/j.oceaneng.2022.111433

[6] Li H, Peng W, Huang C-G, Guedes Soares C. Failure Rate Assessment for Onshore and Floating Offshore Wind Turbines. Journal of Marine Science and Engineering 2022; 10(12): 1965. https://doi.org/10.3390/jmse10121965

[7] Medina-Manuel A, Molina Sánchez R, Souto-Iglesias A. AI-Driven Model Prediction of Motions and Mooring Loads of a Spar Floating Wind Turbine in Waves and Wind. Journal of Marine Science and Engineering 2024; 12(9): 1464. https://doi.org/10.3390/jmse12091464

[8] Palma G, Bardazzi A, Lucarelli A, Pilloton C, Serani A, Lugni C, Diez M. Analysis, Forecasting, and System Identification of a Floating Offshore Wind Turbine Using Dynamic Mode Decomposition. Journal of Marine Science and Engineering 2025; 13(4): 656. https://doi.org/10.3390/jmse13040656

[9] Dong Q, Zhang K, Chen M, Liu H, Luo W, Liu Y, Zhou H, Ren Z. Real-time motion prediction of a 5 MW floating offshore wind turbine using artificial neural networks integrated with time series decomposition. Ocean Engineering 2026; 343: 123301. https://doi.org/10.1016/j.oceaneng.2025.123301

[10] Shi W, Hu L, Lin Z, Zhang L, Wu J, Chai W. Short-term motion prediction of floating offshore wind turbine based on muti-input LSTM neural network. Ocean Engineering 2023; 280: 114558. https://doi.org/10.1016/j.oceaneng.2023.114558

[11] He G, Xue J, Zhao C, Cui T, Liu C. Deep learning based short-term motion prediction of floating wind turbine under shutdown condition. Applied Ocean Research 2024; 151: 104147. https://doi.org/10.1016/j.apor.2024.104147

[12] Yin J, Ding J, Yang Y, Yu J, Ma L, Xie W, Nie D, Bashir M, Liu Q, Li C, Li S. Wave-induced motion prediction of a deepwater floating offshore wind turbine platform based on Bi-LSTM. Ocean Engineering 2025; 315: 119836. https://doi.org/10.1016/j.oceaneng.2024.119836

[13] Song B, Zhou Q, Chang R. Short-term motion prediction of FOWT based on time-frequency feature fusion LSTM combined with signal decomposition methods. Ocean Engineering 2025; 317: 120046. https://doi.org/10.1016/j.oceaneng.2024.120046

[14] Deng S, Ning D, Mayon R. The motion forecasting study of floating offshore wind turbine using self-attention long short-term memory method. Ocean Engineering 2024; 310: 118709. https://doi.org/10.1016/j.oceaneng.2024.118709

[15] Kang B, Park S, Kwon D. Interpretable prediction of floating offshore wind turbine dynamic responses: An attention-based deep learning approach. Ocean Engineering 2025; 335: 121703. https://doi.org/10.1016/j.oceaneng.2025.121703

[16] Fan C, La X, Feng R, Mdemaya FAL, Xu G. Intelligent forecasting of motion responses of offshore floating wind turbines based on artificial intelligence. Ocean Engineering 2026; 349: 124103. https://doi.org/10.1016/j.oceaneng.2025.124103

[17] Chen J, Gunawan D, Taylor PH, McCauley G, Zhao W. Attention-based machine learning for short-term motion prediction of a floating offshore wind turbine. Ocean Engineering 2026; 358: 125780. https://doi.org/10.1016/j.oceaneng.2026.125780

[18] Chen R, Zhang K, Luo M, An Y, Guo L. Deep Learning-Based Prediction of Pitch Response for Floating Offshore Wind Turbines. Journal of Marine Science and Engineering 2024; 12(12): 2198. https://doi.org/10.3390/jmse12122198

[19] Wang Z, Qiao D, Tang G, Wang B, Yan J, Ou J. An identification method of floating wind turbine tower responses using deep learning technology in the monitoring system. Ocean Engineering 2022; 261: 112105. https://doi.org/10.1016/j.oceaneng.2022.112105

[20] Ahn H, Ha Y-J, Kim K-H. Load Evaluation for Tower Design of Large Floating Offshore Wind Turbine System According to Wave Conditions. Energies 2023; 16(4): 1862. https://doi.org/10.3390/en16041862